

Effect of cesium and cerium substitution on the dielectric properties of $\text{CaCu}_3\text{Ti}_4\text{O}_{12}$ ceramics

Worawut Makcharoen^a, Jerapong Tontrakoon^a, Gobwute Rujijanagul^{a,b,*},
David P. Cann^c, Tawee Tunkasiri^{a,d}

^aDepartment of Physics and Materials Science, Chiang Mai University, 50200, Thailand

^bMaterials Science Research Center, Chiang Mai University, 50200, Thailand

^cFaculty of Materials Science, Department of Mechanical Engineering, Oregon State University, Corvallis, OR 97331-8569, USA

^dSchool of Science, Mae Fah Luang University, Chiang Rai 57100, Thailand

Available online 30 April 2011

Abstract

In this study, $\text{CaCu}_3\text{Ti}_4\text{O}_{12}$ (CCTO) ceramics were doped with cesium and cerium atoms to possibly improve the electrical properties of these widely used ceramics. In all cases, pure phase perovskites were produced where cesium doping enhanced the grain growth and cerium doping produced grain growth inhibition. The cesium doping showed an improvement in loss tangent performance, in contrast to the cerium doping which showed a negative result. A high dielectric constant $>15,000$ with a dielectric loss lower than 0.06 was observed for cesium 2.0 mol% doped at high frequencies. These results were related to the change in microstructure and the properties of grain boundary after doping.

© 2011 Elsevier Ltd and Techna Group S.r.l. All rights reserved.

Keywords: A. Grain growth; C. Dielectric properties; D. Perovskites; E. Capacitors

1. Introduction

The high-K ceramic $\text{CaCu}_3\text{Ti}_4\text{O}_{12}$ (CCTO) first discovered by Subramanian et al. [1] exhibits a high dielectric constant over 10,000 at room temperature with temperature independence over the temperature range of ~ 100 – 400 K [2]. For ceramic and thin-film samples at room temperature, typical values of the loss tangent are about 0.2 at 10 kHz [1,3]. The crystal lattice structure of this ceramic is composed of titanate oxide crystals arranged in a cubic structure with an Im3 space group. Since the TiO_6 octahedra are tilted, there is a doubling of the perovskite-like lattice parameter which creates a square planar arrangement of the oxygen around the Cu^{2+} cations [4]. Due to these unusual properties, CCTO ceramics have an electrically heterogeneous structure with mobile charged species which show a Maxwell–Wagner relaxation behavior [5]. The internal interfaces in the polycrystalline CCTO also

give rise to a polarization of the semiconducting grains and insulating grain boundaries based on the internal barrier layer capacitor (IBLC) model [6–8]. There have been numerous reports of cation substitution on the CCTO lattice structure (substitution of Co, Zr, Fe, Ni, Sc and Nb on the B-site, and substitution of La on the A-site) [8–11]. In this report, we studied cation substitution on at both the A-site and B-site of CCTO by doping cesium (Cs) and cerium (Ce). Properties of the samples were investigated and reported.

2. Experimental

The $\text{CaCu}_3\text{Ti}_4\text{O}_{12}$ powders were prepared via a conventional solid state method. For the doping Ce and Cs studies, CeO_2 and Cs_2CO_3 powders were added to CCTO powder at the calcination stage in concentrations of 1.0 and 2.0 mol%. The samples were calcined at 900°C for 2 h and sintered in air at 1100°C for 4 h. Phase formation of the samples was investigated via an X-ray diffraction technique (XRD). The lattice parameter was calculated from the positions of the (2 2 0) and (4 2 2) X-ray diffraction peaks. Density of the ceramic samples was measured using the Archimedes method.

* Corresponding author at: Department of Physics and Materials Science, Chiang Mai University, 50200, Thailand. Tel.: +66 53 943376; fax: +66 53 357512.

E-mail address: rujijanagul@yahoo.com (G. Rujijanagul).

Microstructure of the ceramics was characterized using a SEM (JEOL JSM-5910LV). Average grain sizes of the samples were determined by the intercept count method of ASTM E112, which is based on the number of the grain boundary intersections per unit length [8]. The dielectric constant and the loss tangent were measured with an Agilent 4284A LCR meter.

3. Results and discussion

Fig. 1 illustrates the XRD patterns of CCTO doped with Cs and Ce, which are similar to that of many previous works [3–7]. All samples exhibited a pure perovskite phase with cubic and no symmetry, no contaminating of raw materials or trace of Cs or Ce oxides. The increase in the mole fraction of Cs and Ce shows no evidence of a change in symmetry in the doped ceramics. For the Cs doped samples, the XRD peaks shifted to low angles with increasing Cs concentrations (inset (a) of Fig. 1). This result suggests that Cs doping produced a change in lattice parameter (a). Values of the lattice parameter of the Cs doped samples are shown in Fig. 2, where it increased with increasing Cs concentrations. This indicates that the Cs^{1+} entered into the lattice of CCTO. Comparing the radius of Cs^{1+} ($r_{\text{Cs}^{1+}} = 1.69$) to Ca^{2+} ($r_{\text{Ca}^{2+}} = 1.34$) and Cu^{2+} ($r_{\text{Cu}^{2+}} = 0.57$), the Cs^{1+} ions produce a larger lattice spacing as a substitute to Cu^{2+} . Thus, the increase in lattice parameter for the Cs doped samples (or the XRD peaks shifted in inset (a) of Fig. 1 is the result of substituting Ca^{2+} with Cs^{1+} [9,10]. For the Ce doping, the valance states of this ion are +3 and +4 with ionic radii of 1.06 and 0.97 Å, respectively. Since the ionic radii for Ca and Ti sites are 1.34 and 0.68 Å, respectively, and the lattice parameter for the Ce doped samples remained unchanged, this suggests that either the Ce ions did not enter into the lattices or did not change the average lattice spacing where they did enter. This evidence is similar to the work done by Kwon et al. [12].

The density and shrinkage values versus doping concentration of Ce and Cs are shown in the inset of Fig. 2. The general trend indicates that doping slightly increased the density and shrinkage value. However, the Ce doped samples showed a higher increase. This result indicates that Ce doping helped to

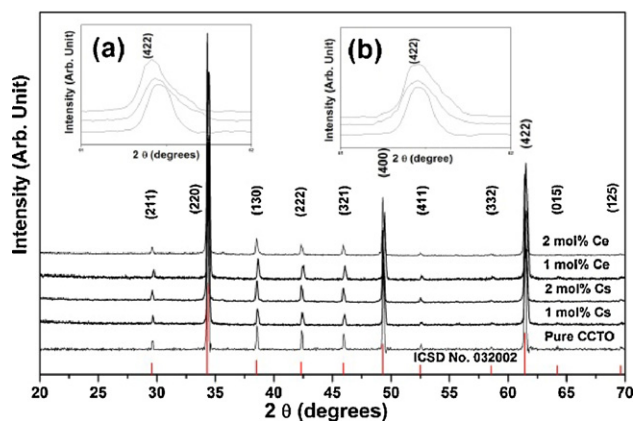


Fig. 1. XRD patterns of pure and doped CCTO ceramics. Insets (a) and (b) show XRD peaks of (4 2 2) planes for Cs and Ce doped CCTO ceramics, respectively.

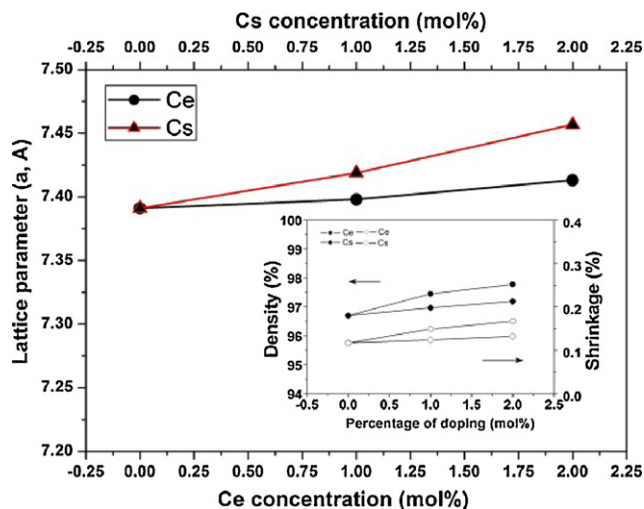


Fig. 2. Lattice constant of doped CCTO ceramics as a function of Cs and Ce concentrations. Inset shows density and shrinkage of doped CCTO ceramics versus Cs and Ce concentrations.

improve the densification of the doped CCTO ceramics. The microstructures of the doped samples are shown in Fig. 3. For the Cs doping, average grain size increased from $\sim 20.4 \mu\text{m}$ for unmodified CCTO (Fig. 3(a)) to $\sim 28.9 \mu\text{m}$ for the 2.0 mol% sample (Fig. 3(b)). In contrast to the Ce doping, a notable decrease in grain size was observed where the 2.0 mol% Ce sample had an average grain size of only $1.9 \mu\text{m}$ (Fig. 3(c)). This result implies that Cs doping promoted grain growth, while Ce doping inhibited grain growth. Furthermore, the reduced grain growth seen with the Ce ions gave rise to a segregation of the doping oxide which formed small scale secondary phases at the grain boundaries without being detected by XRD [10].

Plots of the dielectric properties as a function of temperature (Fig. 4(a)) for the pure CCTO ceramic (100 Hz–500 kHz) illustrated a high dielectric constant with temperature stability over the temperature range of ~ 27 – 60°C of the pure CCTO ceramics, while a tangent loss was less than 0.01 over a range of 27 – 70°C at 10 kHz (Fig. 5(a)). The dielectric constants as a function of temperature of the Cs (Fig. 4(b)) and Ce (Fig. 4(c)) doped CCTO ceramics (100 Hz–500 kHz), indicates that

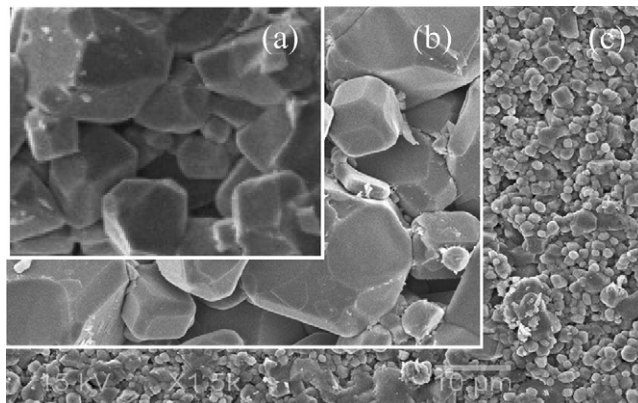


Fig. 3. Fracture surfaces of selected samples: (a) Cs 2.0 mol% doped CCTO and (b) Ce 2.0 mol% doped CCTO.

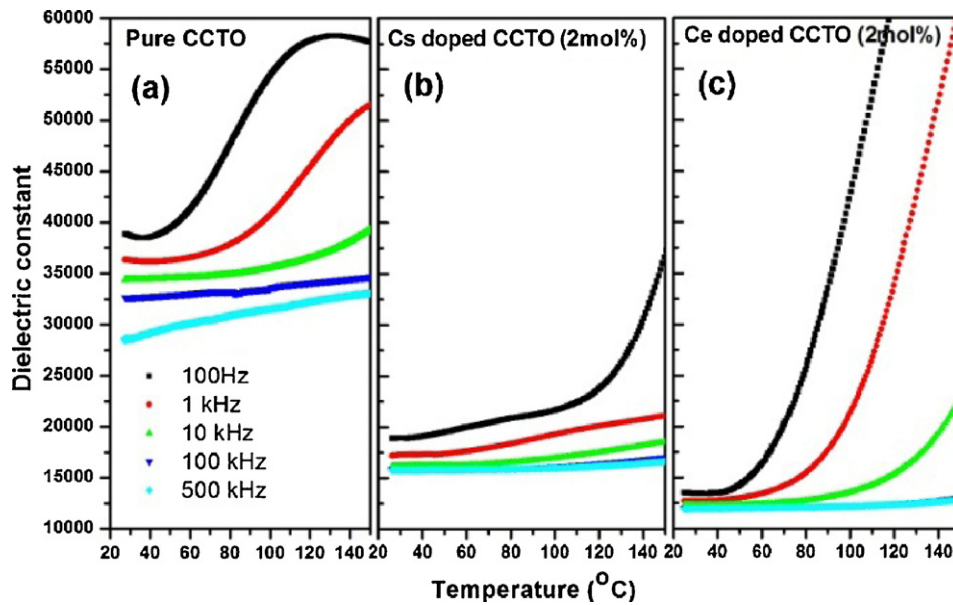


Fig. 4. Dielectric constant as a function of temperature for the ceramics: (a) pure CCTO, (b) Cs 2.0 mol% doped CCTO and (c) Ce 2.0 mol% doped CCTO.

doping of Cs produced a weak of frequency dispersion of the dielectric constant, in contrast to that of the Ce doping where a strong of frequency dispersion was observed. However, all doping conditions exhibited a reduction in dielectric constant at room temperature. This reduction has been observed for many modified CCTO ceramics [9–11].

The values of the loss tangent ($\tan \delta$) as a function of temperature for the Cs and Ce doped CCTO ceramics are shown in Fig. 5(b) and (c), respectively. The Ce samples showed a change of $\tan \delta$ about 150% (from 0.2 at 27 °C to 0.5 at 70 °C) at 1 kHz, while Cs samples exhibited temperature and frequency stability (2% change) over the same temperature range.

The dielectric constants versus frequency plots at room temperature for the Cs and Ce doped ceramics (Fig. 6) show decreasing trend with frequency. Furthermore, a significant decrease in the dielectric constant was observed for the Ce samples comparing to that of the Cs samples. Plots of the loss tangent versus frequency of the pure CCTO ceramic (Fig. 6) at room temperature, show that the loss tangent decreased with increasing frequency up to 1 kHz and then increased with further increases in frequency. However, the additions significantly lowered the rise in loss tangent at high frequencies (>1 kHz), implying a reduced conductivity of the doped ceramics.

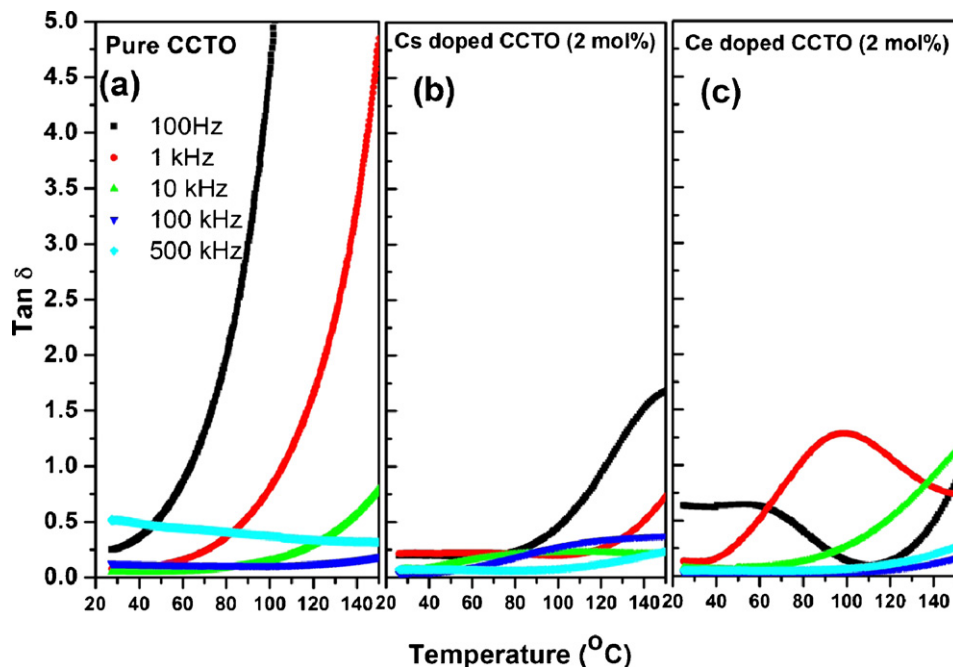


Fig. 5. Loss tangent as a function of temperature of the ceramics: (a) pure CCTO, (b) Cs 2.0 mol% doped CCTO and (c) Ce 2.0 mol% doped CCTO.

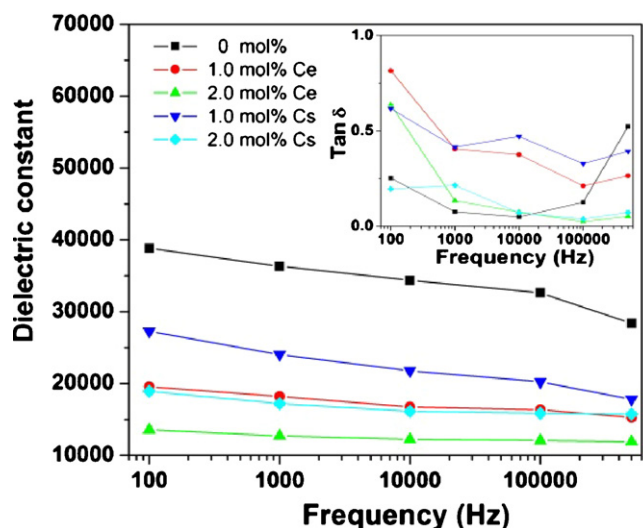


Fig. 6. Dielectric constant as a function of frequency of the ceramics and the inset shows their loss tangent.

From the IBL model [6,7], the CCTO system can be viewed as a circuit consisting of two parallel RC elements connected in series which represent the semiconducting bulk, grain and insulating grain boundary, and grain boundary capacitor. It has also been proposed that the apparent dielectric constant (ϵ'_r) can be related to the grain size (d) and the thickness of the grain boundary (barrier width, t) and internal dielectric constant of the grain boundary (ϵ_{gb}) using the following expression [13]:

$$\epsilon'_r = \epsilon_{gb} \left(\frac{d}{t} \right) \quad (1)$$

In the present work, the reason for the reduction of the dielectric constant of the doped samples are uncertain, but could be linked to the characteristics of the grain boundaries. According to Eq. (1) it is possible that the dielectric constant of the grain boundaries for the doped samples decreased after doping [13] which could cause a decrease in the dielectric constant. Further, it should be noted that the dielectric constant for the Ce doped samples is lower than that the Cs doped samples. This could also result from a decrease in grain size (see also Eq. (1)), as seen in Fig. 3, where a sharp decrease in grain size was recorded for the Ce doped samples.

In the case of the loss tangent behavior of the present samples, the reduction of $\tan \delta$ could be correlated to changes in transport behavior, i.e. an increase in total resistivity of the grain boundaries [14] (which in turn depends on the value of grain boundary resistance) which results in a lowered loss tangent. However, further investigation using different techniques should be performed to clarify the evidence.

4. Conclusions

The properties of Ce and Cs doped CCTO ceramics were investigated for the first time. The pure and modified (CCTO) ceramics were prepared by a conventional solid-state reaction

technique. The different dopant resulted in different grain sizes, where Cs doping promoted grain growth, while Ce doping inhibited grain growth. Although these dopants produced a reduction in the dielectric constant, the dielectric constant after doping was still high especially for Cs doping. The loss tangent performance of the Cs samples was found to improve independently with temperature and frequency. It was proposed that the change in the microstructures could be related to the changes in the dielectric properties.

Acknowledgements

This work was supported by Development and Promotion of Science and Technology Talents Project (DPST), Thailand, Faculty of Science and Graduate School Chiang Mai University, The Thailand Research Fund (TRF) and thank The National Research University Project under Thailand's Office of the Higher Education Commission (OHEC) for financial support.

References

- [1] M.A. Subramanian, D. Li, N. Duan, B.A. Reisner, A.W. Sleight, High dielectric constant in $\text{ACu}_3\text{Ti}_4\text{O}_{12}$ and $\text{ACu}_3\text{Ti}_3\text{FeO}_{12}$ phases, *Journal of Solid State Chemistry* 151 (2000) 323–325.
- [2] A.P. Ramirez, M.A. Subramanian, M. Gardel, G. Blumberg, D. Li, T. Vogt, S.M. Shapiro, Giant dielectric constant response in a copper–titanate, *Solid State Communications* 115 (2000) 217–220.
- [3] W. Si, E.M. Cruz, P.D. Johnson, P.W. Barnes, P. Woodward, A.P. Ramirez, Epitaxial thin films of the giant-dielectric-constant material $\text{CaCu}_3\text{Ti}_4\text{O}_{12}$ grown by pulsed-laser deposition, *Applied Physics Letters* 81 (2002) 2056.
- [4] Y. Lin, Y.B. Chen, T. Garret, S.W. Liu, C.L. Chen, L. Chen, R.P. Bontchev, A. Jacobson, J.C. Jiang, E.I. Meletis, J. Horwitz, H.D. Wu, Epitaxial growth of dielectric $\text{CaCu}_3\text{Ti}_4\text{O}_{12}$ thin films on (0 0 1) LaAlO_3 by pulsed laser deposition, *Applied Physics Letters* 81 (2002) 631.
- [5] P. Lunkenheimer, V. Bobnar, A.V. Pronin, A.I. Ritus, A.A. Volkov, A. Loidl, Origin of apparent colossal dielectric constants, *Physical Review B* 66 (2002) 052105.
- [6] D.C. Sinclair, T.B. Adams, F.D. Morrison, A.R. West, $\text{CaCu}_3\text{Ti}_4\text{O}_{12}$: one-step internal barrier layer capacitor, *Applied Physics Letters* 80 (2002) 2153.
- [7] T.B. Adams, D.C. Sinclair, A.R. West, Characterization of grain boundary impedances in fine- and coarse-grained $\text{CaCu}_3\text{Ti}_4\text{O}_{12}$ ceramics, *Advanced Materials* 14 (2002) 1321.
- [8] G.F. Vander Voort, A.M. Gokhale, Comments on Grain size measurements, *Scripta Materialia* 26 (1992) 1655.
- [9] R.D. Shannon, C.T. Prewitt, Revised values of effective ionic radii, *Acta Crystallographica Section B* 26 (1970) 1046–1048.
- [10] Chun-Hong Mu, Peng Liu, Ying He, Jian-Ping Zhou, Huai-Wu Zhang, An effective method to decrease dielectric loss of $\text{CaCu}_3\text{Ti}_4\text{O}_{12}$ ceramics, *Journal of Alloys and Compounds* 471 (2009) 137–141.
- [11] S.Y. Chung, S.I. Lee, J.H. Choi, S.Y. Choi, Initial cation stoichiometry and current–voltage behavior in Sc-doped calcium copper titanate, *Applied Physics Letters* 89 (2006).
- [12] S. Kwon, C.-C. Huang, E.A. Patterson, D.P. Cann, The effect of Cr_2O_3 , Nb_2O_5 and ZrO_2 doping on the dielectric properties of $\text{CaCu}_3\text{Ti}_4\text{O}_{12}$, *Materials Letters* 62 (2008) 633–636.
- [13] F. Amaral, M.A. Valente, L.C. Costa, Dielectric properties of $\text{CaCu}_3\text{Ti}_4\text{O}_{12}$ (CCTO) doped with GeO_2 , *Journal of Non-Crystalline Solids* 356 (2010) 822–827.
- [14] L. Ni, X.M. Chen, X.Q. Liu, R.Z. Hou, Microstructure-dependent giant. Dielectric response in $\text{CaCu}_3\text{Ti}_4\text{O}_{12}$ ceramics, *Solid State Communications* 139 (2006) 45–50.